# High genetic load without purging in a diverse species-at-risk

**Rebecca S. Taylor[1*], Micheline Manseau[1], Sonesinh Keobouasone[1], Peng Liu[1], Gabriela Mastromonaco[2], Kirsten Solmundson[3], Allicia Kelly[4], Nicholas C. Larter[5], Mary Gamberg[6], Helen Schwantje[7], Caeley Thacker[8], Jean Polfus[9], Leon Andrew[10], Dave Hervieux[11], Deborah Simmons[10], Paul J. Wilson[3]**

[1]Landscape Science and Technology, Environment and Climate Change Canada, Ottawa, Canada. [2]Toronto Zoo, Toronto, Canada. [3]Biology Department, Trent University, Peterborough, Ontario, Canada. [4]Department of Environment and Natural Resources, Government of Northwest Territories, Fort Smith, Northwest Territories, Canada. [5]Retired, formally Department of Environment and Natural Resources, Government of Northwest Territories, Fort Simpson, Northwest Territories, Canada. [6]Gamberg Consulting, Whitehorse, Yukon, Canada. [7]Retired, formally British Columbia ministry of Forest, Lands, Natural Resource Operations, and Rural Development, Nanaimo, British Columbia, Canada. [8]British Columbia ministry of Forest, Lands, Natural Resource Operations, and Rural Development, Nanaimo, British Columbia, Canada. [9]Canadian Wildlife Service - Pacific Region, Environment and Climate Change Canada, Kelowna, British Columbia, Canada. [10]ehdzo Got'ı̨nęGots'ę́Nákedı (Sahtú Renewable Resources Board), Tuĺıt'a, Northwest Territories, Canada. [11]Department of Environment and Parks, Government of Alberta, Grande Prairie, Alberta, Canada.

*Correspondance: rebecca.taylor@ec.gc.ca

**SUMMARY**

High intra-specific genetic diversity is associated with adaptive potential which is key for resilience to global change. However, high variation may also support deleterious alleles through genetic load, unless purged, thereby increasing the risk of inbreeding depression if population sizes decrease rapidly. Purging of deleterious variation has now been demonstrated in some threatened species. However, less is known about the costs of population declines and inbreeding in species with large population sizes and high genetic diversity even though this encompasses many species globally that have or are expected to undergo rapid population declines. Caribou is a species of ecological and cultural significance in North America with a continental-wide distribution supporting extensive phenotypic variation, but with some populations undergoing significant declines resulting in their at-risk status in Canada. We assessed intra-specific genetic variation, adaptive divergence, inbreeding, and genetic load across populations with different demographic histories using an annotated chromosome-scale reference genome and 66 whole genome sequences. We found high genetic diversity and nine phylogenomic lineages across the continent with adaptive diversification of genes, but also high genetic load among lineages. We also found highly divergent levels of inbreeding across individuals including the loss of alleles by drift (genetic erosion) but not purging, likely due to rapid population declines not allowing time for purging of deleterious alleles. As a result, further inbreeding may need to be mitigated through conservation efforts. Our results highlight the 'double-edged sword' of genetic diversity that may be representative of other species-at-risk affected by anthropogenic activities.

**KEYWORDS**

Caribou, genetic diversity, inbreeding, intra-specific variation, mutational load

## INTRODUCTION

Intra-specific diversity is crucial for adaptive potential and resilience of species under environmental changes (Andrello et al., 2022; Carvalho et al., 2017; O'Brien et al., 2022; Hoban et al., 2022;). Therefore, understanding the drivers of intra-specific genetic variation and its interplay with adaptive divergence is essential to understanding how current species respond to environmental variations (Des Roches et al., 2021; Leigh et al., 2021; Yiming et al., 2021). Conversely, there is growing evidence suggesting that a larger genetic load is present in populations with high genetic diversity (Bertorelle et al. 2022; van Oosterhout et al. preprint). Recent research on threatened populations or species with low genetic diversity has demonstrated the purging of deleterious genetic variation due to the maintenance of small population sizes, for example, in the Sumatran rhinoceros (vonSeth et al. 2022), the kākāpō (Dussex et al. 2021), Alpine ibex (Grossen et al. 2020), and Indian tigers (Khan et al. 2021), with some threatened species nevertheless developing inbreeding depression likely due to rapid declines and historical demography, for example, in killer whales (Kardos et al. 2023) and Scandinavian wolves (Smeds and Ellegren, 2022).

Less is known about the costs of population declines and inbreeding in species with large population sizes and high genetic diversity (Fairmount et al. 2023), even though this encompasses many species globally that have not maintained small population sizes but will likely undergo rapid declines and fragmentation into isolated populations due to anthropogenic impacts. Such species with large historical effective populations sizes are expected to have high genetic load (Bertorelle et al. 2022; van Oosterhout et al. preprint) and may decline too rapidly to purge deleterious variation. We investigate these processes in an example of such a species, caribou (*Rangifer tarandus*), a wide-spread and diverse species-at-risk.

Caribou (known as reindeer in Eurasia) is a highly mobile keystone species with a continental-wide distribution, ranging from the high Arctic to the boreal forests, and spanning from the east to the west coast of North America (COSEWIC, 2011; Figure 1). Across its range caribou have a large amount of

70 phenotypic and genetic variation and have been divided into 12 conservation units, known as
71 Designatable Units (DUs), by the Committee on the Status of Endangered Wildlife in Canada (COSEWIC,
72 2011; Figure 1). Caribou DUs face threats including habitat destruction and climate change (Festa-
73 Bianchet et al., 2011; Vors & Boyce, 2009; Weckworth et al., 2018), with nine DUs currently listed as
74 endangered or threatened, two as special concern, and one that is extinct (COSEWIC, 2011-2017).
75 Globally, in 2015 the species changed from Least Concern to Vulnerable on the IUCN Red List due to the
76 species undergoing a 40% decline over three generations (IUCN Red List).

77 We investigated intra-specific lineage diversity, genetic variation, adaptive diversification,
78 inbreeding extent, and mutational load in caribou across North America and Greenland using whole
79 genome sequencing thus undertaking a comprehensive reconstruction of intra-specific caribou diversity.
80 We first assess intra-specific diversity and the processes that may have led to high genetic variation, as
81 well as adaptive diversification. We then characterize inbreeding and compare genetic load in individuals
82 with different demographic histories (high vs low inbreeding) to understand the potential impact of rapid
83 population declines on genetic diversity as well as on deleterious variation in a genetically and
84 phenotypically diverse species. Since many species have not maintained small population sizes over time
85 but have or are expected to undergo rapid population declines due to anthropogenic impacts including
86 climate change, it becomes imperative to better understand the many facets of genetic diversity and
87 ultimately ensure the long-term resilience of our wild species.

88

89 **RESULTS AND DISCUSSION**

90 We assembled a new caribou reference genome with a contig N50 of 32.82 KB, scaffold N50 of 64.42
91 MB, and an L50 of 14, with 99.5% of the assembly being on 36 scaffolds. As the chromosome number is
92 70 for the species (34 autosome pairs plus the sex chromosomes; Gripenberg et al. 1986), this likely

93 represents a chromosome-scale assembly. We then used RNA-seq data to perform a high-quality
94 annotation of the genome, which identified the locations of 34,407 protein-coding genes. Using 66 re-
95 sequenced genomes from across North America and Greenland representing eight Designatable Units
96 (DUs) and 33 subpopulations (Figure 1; Table S1 and S2), phylogenomic reconstruction using two
97 different methods was generally consistent and separated caribou into nine major lineages, which were
98 not concordant with DU designations (Figure 2a; Figure S1). We reconstructed the major mitochondrial
99 lineages known from previous studies (Weckworth et al. 2012); the North American lineage (NAL) and
100 the larger and more diverse Beringian-Eurasian lineage (BEL) which contains eight lineages in our results
101 (Figure 2a; Figure S1). The only discordance between our two reconstructions was that the NWB lineage
102 was basal to the PMG lineage instead of a sister group, and that the BRG lineage individuals were within
103 (although on the outside) of the ARC group instead of a sister lineage in the SNP based reconstruction
104 (Figure S2). We show the results based on the more powerful method using full sequence data (Figure
105 2a), especially given the large differences between BRG and ARC individuals in further analyses. The
106 principal component analysis (PCA) is also concordant with the phylogenomic results separating into
107 three major clusters on PC1: the NAL individuals, NWB, PMG and CSM individuals, and the three major
108 northern mountain lineages (GRA, NM1, and NM2; Figure S3). On PC2, the BRG and ARC lineages
109 separate (Supplementary Figure 3).

110 As well as exploring lineage diversity, we calculated individual genetic diversity, θ, an
111 approximation of heterozygosity under the infinite sites model (vonSeth et al. 2022; Haubold et al. 2010;
112 Foote et al. 2021). We found overall high heterozygosity in caribou, although with some variation among
113 individuals (overall mean of 0.0030, range of 0.0012 to 0.0036; Figure 2b; Figure S4). Some individuals
114 from within the NAL and ARC lineages had lower diversity than the others, with the ARC lineage mean θ
115 at 0.0024 and the NAL at 0.0028 compared to the mean of all others at 0.0031 (Figure 2b; Figure S4).
116 When compared to other mammal species where genome-wide heterozygosity has been calculated, our

117 mean is around some of the highest heterozygosity values (see Figure 3 in Morin et al. 2020),
118 demonstrating a high genetic diversity, as well as high phylogenetic lineage diversity, in caribou.

119 To measure introgression among the reconstructed lineages, we used D and f4-ratio tests, which
120 control for incomplete lineage sorting. These statistics gave many significant signatures of introgression
121 between groups (Supplementary Material: Introgression statistics). We then calculated the f-branch
122 statistic, which accounts for many correlated signatures of introgression using the f4-ratio statistics to
123 show when along the phylogeny introgression occurred, and whether the gene flow event was into an
124 ancestral group. The f-branch results indicated widespread introgression between lineages, particularly
125 between NAL and the ancestor of NWB and PMG lineages, and multiple lineages into CSM, the ancestor
126 of NM1 and NM2, NM2, and BRG (Figure 3a). In contrast, some lineages show only a small amount or
127 even a lack of gene flow (with the caveat that sister groups cannot be tested for gene flow using ABBA
128 BABA tests). For example, no lineage shows gene flow into the ARC, GRA, or NM1 caribou lineages
129 (Figure 3a). To explore potential introgression between sister lineages, we visualized 'admixture graphs'
130 in SplitsTree. Unsurprisingly these graphs show some phylogenetic uncertainty, putatively due to gene
131 flow, within lineages (Supplementary Figure 5). We also see potential signals of introgression between
132 the NWB, PMG, and CSM lineages, which may help to explain the placement of the PMG individuals next
133 to the NWB lineage in the phylogenetic reconstruction, as well as some potential introgression between
134 the three major northern mountain lineages (GRA, NM1, and NM2).

135 Altogether our results, reconstructing continent-wide whole genome phylogenomic history for
136 the first time, point towards a high level of intra-specific diversity in caribou, with some strong signals of
137 introgression among many of the lineages. Our results build on previous studies showing high genetic
138 diversity in caribou, for example large numbers of mitochondrial haplotypes (Weckworth et al. 2012;
139 Polfus et al. 2017; Taylor et al. 2021) and high diversity in microsatellite loci (Boulet et al. 2007;
140 McLoughlin et al. 2004; Zittlau et al. 1998). The reasons behind the high diversity and number of intra-

141 specific lineages are likely multi-faceted. The large Beringian refugium, where the individuals from the
142 BEL lineages spent the glacial cycles of the Quaternary, harboured high levels of genetic diversity for
143 some, particularly cold adapted, species such as caribou (Galbreath et al. 2011; Dussex et al. 2020), and
144 is reflected in the large diversity in the BEL vs the NAL caribou (Fig 2a). Post-glacial expansion out of
145 refugia can lead to genetic bottlenecks and low diversity further away from the refugial populations
146 (Roberts and Hamann 2015). However, repeated secondary contact and admixture between glacial
147 lineages can increase genetic diversity (Petit et al. 2003; Alcala and Vuilleumier 2014), in a similar
148 mechanism to the 'glacial pulse model' which describes how lineage fusion during glacial cycles can be a
149 source of intra-specific lineage diversity (Maier et al. 2019). Indeed, well-known determinants of
150 diversification during adaptive radiations include high standing variation, gene flow, and habitat to
151 diversify into (Berner and Salzburger 2015), all of which are true for caribou post-glacial recolonizations.

152 The life history of caribou is also particularly conducive to the formation of high intra-specific
153 variation. Deer species have a high intrinsic rate of increase and dispersal capabilities (Latch et al. 2009).
154 High vagility means caribou were able to undergo range shifts and quickly recolonize habitat once ice
155 sheets recede, or use ice-free corridors (Latch et al. 2009; Dussex et al. 2020; Taylor et al. 2021),
156 facilitating repeated refugial lineage contact potentially increasing genetic diversity as described above.
157 The same processes leading to high genetic variation will likely also have increased standing
158 adaptive variation in caribou. We used the branch model approach in the codeml module of PAML (Yang
159 2007) to calculate the ratio of synonymous to non-synonymous mutations (dN/dS ratio) within genes.
160 The program then performs likelihood ratio tests to elucidate whether the 'focal' branch has a
161 significantly different ratio from the rest of the phylogenetic tree and is thus putatively a rapidly evolving
162 gene within that branch when compared to the overall phylogeny. We ran each of the nine major linages
163 from our whole genome phylogeny as the focal branch to find those rapidly evolving genes significant to
164 each, thus potentially involved in the adaptive diversification of the lineage.

165 We found a number of rapidly evolving genes within each lineage (Table S3; Supplementary
166 Material: CodeML). However, contrary to our expectations to find more lineage specific genes in those
167 with lower levels of introgression (as for example in the ARC lineage), we found similar numbers of
168 statistically significant genes after Bonferroni correction for each both overall ($X^2 = 3.058$, df = 8, p =
169 0.931) and for the genes unique to each lineage ($X^2 = 8.142$, df = 8, p = 0.420; Table S3). This could be
170 due to the relatively short time scale of the diversification (all within ~120,000 years; Taylor et al. 2021)
171 limiting the number of genes within each lineage with a high dN/dS ratio. It could also be due to the high
172 level of overall connectivity (introgression) detected among lineages limiting the significant genes
173 resulting from the codeml approach which scans for genes with a strong signature of positive selection
174 when compared to the rest of the phylogeny (i.e. not detecting genes that are important for all or many
175 caribou lineages). There was overlap in the genes that pulled out as significant for each lineage
176 (Supplementary Material: CodeML), which may be indicative of the diversification occurring from a large
177 pool of standing genetic variation, which is known to be a driver of diversification during adaptive
178 radiations (Berner et al. 2015).
179 We used the codeml approach due to our questions relating to the diversification among caribou
180 lineages, as well as our phylogenomic framework, and have thus characterized some genes putatively
181 involved in the differential adaptation of the caribou lineages (Supplementary Material: CodeML). We
182 performed gene ontology (GO) analyses to assign functional categories to the genes under both
183 'biological process' and 'molecular function' and found a number of processes represented in the
184 significant genes such as immune processes, stress responses, carbohydrate binding, amongst many
185 others (Supplementary Material: Gene ontology for all GO terms for each lineage). We then performed
186 enrichment analyses for each lineage, also under both 'biological process' and 'molecular function', in
187 order to find specific pathways containing multiple genes with signatures of rapid evolution. We found
188 that caribou lineages had different numbers of enriched pathways, with some lineages showing a

189 significantly larger number compared to the others ($X^2$ = 112.71, df = 8, p = 2.2e-16; Figure 3b). In
190 particular, the CSM, NWB, and PMG lineages all show high numbers of enriched pathways. These
191 lineages also show some of the highest signatures of introgression, with the CSM lineage showing high
192 introgression from multiple lineages, as well as into the PMG lineage (Figure 3a), and with the admixture
193 graphs showing potential gene flow between the CSM, NWB, and PMG lineages (Figure S5). Similarly, the
194 NM2 lineage also shows a high number of enriched pathways (Figure 3b) and has signatures of
195 introgression from many other lineages (Figure 3a) as well as with the NM1 and GRA lineages (Figure S5).
196 Gene flow may further enhance the variability of functional pathways by exchanging gene variants
197 among lineages creating new combinations, thereby increasing adaptive potential. These combinational
198 pathway changes may well facilitate expression levels and timing prompting adaptation to the range of
199 ecozones inhabited by caribou and the larger *Rangifer* range (Weldenegodguad et al. 2021). It is known
200 that gene flow can facilitate adaptive diversification, as well as inflating standing genetic variation as a
201 whole (Streicher et al. 2014; Berner et al. 2015; Lexer et al. 2016) and may have been a driver of
202 adaptive diversification in these caribou lineages.

203 Despite their abundance as well as their high phenotypic, lineage, and genetic diversity (Figure
204 2) with overall high introgression (Figure 3a), and differential adaptive genetic diversity of caribou (Figure
205 3b; Table S3), some populations have undergone dramatic declines in recent years. For example, the
206 range of boreal caribou in Ontario (NAL lineage) has become disjunct and the populations along the
207 southern edge of the distribution (Lake Superior) have declined to very small numbers of individuals and
208 have already been shown to have elevated signatures of inbreeding (Solmundson et al. 2023). Other
209 populations, for example the Qamanirijuaq barren-ground caribou (BRG lineage) are decreasing but are
210 still in large numbers (~250,000 individuals for the Qamanirijuaq caribou; COSEWIC, 2016), while some,
211 for example northern mountain caribou from the Redstone (NM1 lineage) and Aishihik (GRA lineage)
212 have remained stable or are increasing (COSEWIC 2014; See Supplementary Material for more detail on

213 what is known about the effective and census population sizes of each of the sampled caribou
214 subpopulations). We measured the effect of demography on signatures of inbreeding using runs of
215 homozygosity (ROH) estimation, and found varied levels of inbreeding across individuals ranging from
216 FROH (proportion of the genome in ROH) of 1% or less in the barren-ground caribou in the BRG and GRA
217 lineages, up to around 56% in caribou from Kangerlussuaq in Greenland (ARC lineage; Figure 4; Figure
218 S6), a number comparable to some of the most endangered species such as southern resident killer
219 whales (Kardos et al. 2023), kākāpō (Dussex et al. 2021) and Indian tigers (Kahn et al. 2021). When we
220 look at the longest ROHs (over 1 million bases long) indicating strong signatures of inbreeding, we see
221 the most in the boreal caribou from the disjunct and most southern part of the range in Ontario (NAL
222 lineage), Itcha-Ilgachuz caribou from British Columbia (CSM lineage), Aishihik caribou from the Yukon
223 (GRA lineage), and Kangerlussuaq caribou from Greenland (ARC lineage; Figure 4; Figure S7). The most
224 inbred caribou are generally from the most northern or southern portions of the distribution where
225 genetic erosion due an extreme environment (north) or anthropogenic disturbance (south) are the
226 strongest (Solmundson et al. 2023) with the exception of the Aishihik caribou which are known to have
227 been introgressed with introduced reindeer (Taylor et al. 2021). For the Itcha-Ilgachuz caribou, declines
228 were seen in the 1900s potentially due to hunting, with the population recovering after the 1970s (Seip
229 and Chichowski 1994; Ministry of Forests, Lands, Natural Resource Operations and Rural Development,
230 2018), although is once again declining more recently (COSEWIC, 2011-2017). The Kangerlussuaq caribou
231 in Greenland are known to have undergone and strong decline, maintaining low population sizes
232 between 1845 and the 1950s (Cuyler et al. 2002).

233 Overall, our results demonstrate that different demographic histories have had a dramatic
234 impact on levels of inbreeding and so we investigated genetic load and whether deleterious variation has
235 been purged in the highly inbred compared to non-inbred individuals. Using multispecies comparisons
236 and genomic evolutionary rate profiling (GERP; Davydov et al. 2010), we find fewer derived sites with

237 positive GERP scores and scores over two (at the top end of the score range in our dataset) indicating
238 fewer putatively deleterious variants in the most inbred individuals (Figure 5a and c; Table S4). However,
239 if this was due to purging we would hypothesise the average GERP score of those derived sites to be
240 lower in inbred individuals, but we find no difference in the average score of all positive sites or of the
241 sites with a score over 2 (Figure 5b and c; Table S4) indicating loss of alleles through genetic drift but not
242 purging. Similarly, using our new genome annotation we found fewer derived loss of function (LOF) and
243 high impact alleles in the more inbred individuals, but the pattern is the same for moderate and low
244 impact alleles (Figure 6; Table S4). Our results follow the 'drift only' pattern described in Dussex et al.
245 (2023) and thus indicate genomic erosion and loss of overall diversity through drift without preferential
246 purging of deleterious variation. This is in contrast with other species found to have such a high FROH as
247 our most inbred individuals (i.e., 22-42% in disjunct Ontario boreal caribou and 56% in Kangerlussuaq
248 caribou) which have shown to have purged at least some deleterious variation (e.g., Kardos et al. 2023;
249 Dussex et al. 2021; Kahn et al. 2021).

250 The high impact alleles we uncovered are almost all heterozygous and therefore represent
251 masked load (Bertorelle et al. 2022; van Oosterhout et al. preprint), although we did use strict filtering
252 (e.g., the removal of all sites with any missing data) in order to be conservative and so the numbers are
253 likely underestimates of the 'true' load. Even so, we have 11 homozygous high impact alleles
254 representing realized load (Bertorelle et al. 2022; van Oosterhout et al. preprint), eight of which are in
255 the NAL lineage which has high overall inbreeding levels (Table S4), indicating the possibility of these
256 caribou becoming susceptible to inbreeding depression.

257 It is difficult to compare load across studies due to differences in genome annotations and data
258 filtering, as well as the multi-species alignment used for GERP analysis. However, our data indicate
259 hundreds of high impact alleles present in each individual (between 198 and 610) as well as thousands
260 of moderate impact alleles representing for example, missense mutations (Table S4), representing a large

261 overall genetic load in caribou. This is not surprising given their high historical effective population sizes
262 (Taylor et al. 2021), high phenotypic diversity (COSEWIC), and high genetic and intra-specific lineage
263 diversity and gene flow we reconstructed here.

264 Preserving the high genetic diversity of caribou, indicated here by the divergent intra-specific
265 lineages and high heterozygosity (Figure 2) and the evidence of differential adaptive variation between
266 lineages (Figure 3; Table S3), may be important for the persistence of caribou and their ability to adapt to
267 environmental changes (Carvalho et al. 2017; Andrello et al. 2022). Given that small populations have
268 not purged deleterious variation, maintaining connectivity between populations and lineages is
269 important as introgression appears to be a driver of genetic variation (Figure 3), allowing movement of
270 adaptive genes (Hanson et al. 2019) and preventing an increase in realized genetic load as has been
271 recommended in other species (e.g., Smeds and Ellegren, 2022). As some of these populations have
272 recently declined to small census sizes, particular attention should be put in assessing the potential
273 impact of inbreeding on current and future trends. Important next steps will include increasing the
274 sample sizes within each subpopulation to enable more detailed population scale analyses, such as
275 recent effective population size reconstructions, a task which will require considerable sequencing effort
276 across such a vast range and will likely need to be undertaken at a regional scale.

277

278 **Conservation implications**

279 Much has been published recently in understanding the impacts of low genetic variation and genomic
280 load associated with inbreeding in species with relatively long-term overall low population size (VonSeth
281 et al. 2022; Dussex et al. 2021, Grossen et al. 2020; Khan et al. 2021; Mathur et al. 2023, Kleinman-Ruiz
282 et al. 2022, Xie et al. 2021). However, a different category of at-risk species, such as caribou, sees large
283 effective populations sizes declining thereby manifesting a trade-off of supporting higher potentially

284 adaptive genetic variation, but with the maintenance of non-purged detrimental genetic load with
285 increased probability of expression as such declines occur: the “double edged sword” of higher genetic
286 diversity. We therefore need studies across taxa presenting different demographic histories to enable
287 improved prediction of how a wider variety of species will be affected by population declines.

288 High genetic load is likely supported in many widespread and diverse species with similar
289 demographic histories to caribou (van Oosterhout et al. preprint) that are perhaps not yet threatened
290 but that have started or will inevitably be impacted by anthropogenic activities such as habitat loss and
291 climate change into the future. As caribou have already begun to be impacted and undergo rapid
292 declines in some areas, the genetic erosion and lack of purging even with high inbreeding levels might
293 foreshadow what will occur in these other taxa.

294

295 **METHODS**

296 **Caribou chromosome scale reference genome assembly and annotation**

297 To ensure high quality, contiguous DNA for chromosome-scale reference genome assembly, fibroblast
298 cells were taken from caribou at Toronto Zoo and cultured in T-75 flasks. Firstly, we pre-warmed DMEM1,
299 DMEM3 and trypsin to 37-38 °C, then discarded media and rinsed each T-75 flask with 5 ml of DMEM1.
300 We discarded the media, and added 3 ml of trypsin to each flask and incubate at 38 °C for 2 min. We
301 checked to see that cells had lifted, and then added 9 ml of DMEM3 to each flask, rinsed the flask
302 growing surface to retrieve as many cells as possible and transferred the entire volume to a 15 ml tube,
303 leaving 4 x 15 ml tubes, 2 for each animal. We then centrifuged at 200 x g for 5 min to pellet cells,
304 discarded supernatant and re-suspend pellet in 0.8 ml of PBS. We combined pellets for each individual
305 together in a 2 ml tube, centrifuged in microcentrifuge at 200 x g for 5 min, and discarded the
306 supernatant. The samples were then flash frozen using liquid nitrogen and transferred to a dry shipper
307 and shipped to Dovetail Genomics as we wanted to improve our previous assembly also sequenced by

308 Dovetail Genomics (Taylor et al., 2019), by further scaffolding using Omni-C libraries (Putnam et al.,
309 2016; Yamaguchi et al., 2021). Cells were cultured as above and shipped to Genewiz (Azenta Life
310 Sciences) for RNA sequencing for the annotation. Full details of the sequencing, assembly, and
311 annotation as performed by Dovetail Genomics are available in the Supplementary Material.

312

313 **Re-sequenced whole genome sequences**

314 Whole genome sequences of 50 individuals used in this study are available on the National Centre for
315 Biotechnology (NCBI) under BioProject Accession numbers PRJNA634908, PRJNA694662, PRJNA754521,
316 and PRJNA984705 (Table S2; Taylor et al., 2020; Taylor et al., 2021; Taylor et al., 2022). For this study, we
317 sequenced 16 new genomes (Figure 1; Table S2) using the same protocols as before (Taylor et al., 2020;
318 Taylor et al., 2021; details in the Supplementary Material).

319 All code used to filter and map re-sequenced genomes, as well as for downstream analyses, can
320 be found on GitHub (https://github.com/BeckySTaylor/Phylogenomic_Analyses). Raw reads for all 66
321 individuals were cleaned using Trimmomatic version 0.38 (Bolger et al., 2014) using a sliding window of 4
322 base pairs to trim once phred score dropped below 15. We aligned all trimmed reads to the new
323 reference genome, which we first indexed using Bowtie2 version 2.3.0 (Langmead & Salzberg, 2012). We
324 converted the SAM files to BAM files and sorted them using Samtools version 1.5 (Li et al., 2009), and
325 then added read group information using GATK4 (McKenna et al., 2010). Using GATK4, we removed
326 duplicates and used 'HaplotypeCaller' to call variants and produce a variant calling format (VCF) file. We
327 used the 'CombineGVCFs' function, followed by 'GenotypeGVCFs' to produce a VCF file containing all
328 individuals. We did two rounds of filtering on the VCF file using VCFtools version 0.1.16 (Danecek et al.,
329 2011). We removed indels, and any site low-quality genotype calls (minGQ) and low-quality sites (minQ),
330 with scores below 20, as well as any site with a depth of less than five or more than double the mean
331 depth of all genomes, filtering to remove sites with a depth of more than 55. For the second round of

332 filtering, we made two VCF files; one made using a more 'stringent' filter to remove all missing data, and
333 a 'less stringent' filter to removed sites with more than 5% missing data, resulting in 17,595,673 and
334 41,321,354 SNPs respectively.

335 We also downloaded the raw reads for five Fennoscandian Wild Tundra reindeer genomes to use
336 as outgroups for phylogenomic analyses (ID numbers NMBU 38-42 from Weldenegodguad et al., 2020,
337 European Nucleotide Archive accession PRJEB37216). We mapped and filtered the reads as above, as
338 well as producing a VCF file containing these and the 66 caribou genomes. We filtered the VCF file in
339 VCFtools as above, this time removing sites with a depth over 48 (double the mean of this data set) and
340 removing sites with more than 5% missing data, we had 16,119,954 SNPs.

341 We chose downstream analyses, outlined below, which are appropriate for our sampling across
342 the very large caribou range, which included one or two samples from each of 33 different caribou
343 subpopulations, representing eight DUs (See supplementary materials and Table S1 for more detail on
344 our sampled populations and what is known about their effective and census population sizes). The
345 majority of our analyses are thus those which do not rely on grouping samples together and give
346 individual metrics, with the exception of the CodeML and introgression statistics where we are
347 specifically interested in metrics at a phylogenomic scale. Future work will aim to increase sample size
348 within each subpopulation to enable analyses such as recent Ne reconstruction which need more than 1-
349 2 samples to run and cannot be done grouping samples with genetic differentiation between them (e.g.,
350 using GONE or StairwayPlot2), as well as other analyses requiring the site frequency spectrum. Given the
351 extremely large range of caribou and high number of subpopulations, this will require a huge sequencing
352 effort and likely need to be done at a more regional scale. Many of the results we present here are,
353 however, plotted grouped by lineage for clarity, but all statistics for each individual are given in the
354 supplementary materials.

355

356 **Whole genome phylogenomic reconstruction**

357 For the phylogenomic reconstruction, we used IQtree version 1.6.12 (Nguyenet al., 2015). First, we made
358 a consensus fasta file for each individual from the VCF file which included the reindeer using the
359 'consensus' command in BCFtools. We found that running IQtree on the full genome sequences required
360 too much computational power, so we split the genome into seven sections of close to 300 million base
361 pairs, made a phylogeny with each, and then made a consensus tree as follows. Firstly, we used the
362 'CSplit' command to split each individual fasta file into one file per scaffold, retaining the files for
363 scaffolds 1-36 (which contains ~99% of the reference genome, see results). We concatenated all caribou
364 individuals together for each scaffold, and ran each scaffold from 1-36 in Model Finder in IQtree. Using
365 the Bayesian Information Criterion, Model Finder gave the model TVM+F+I+G4 for all scaffolds apart
366 from 33 where it selected GTR+F+I+G4. For all scaffolds the scores for these two models were close, and
367 for scaffold 33 the likelihood score for the two models was similar (111,917,190.538 and
368 111,917,210.388), and so when concatenating the scaffolds, we used TVM+F+I+G4 for the full
369 phylogenomic run.

370 To run the phylogenomic analysis, we then concatenated scaffolds together for each individual
371 into seven fasta files of roughly 300 million base pairs (scaffolds 1-3, 4-7, 8-11, 12-16, 17-21, 22-27, 28-
372 35), excluding scaffold 36 which is putatively part of the X chromosome based on the presence of known
373 X chromosome genes on that scaffold (Galloway et al., 1996; Liu et al., 2019). We then reformatted each
374 so that the sequence was on one line using 'awk' and 'grep' commands, and then concatenated all
375 individuals together into one file, including the reindeer, for each of the seven sections so we had one
376 fasta file with all individuals for each of the ~300 million base pair regions. We then ran IQtree using
377 100,000 bootstraps to obtain branch supports (-bb command) (Hoang et al., 2018) to produce the
378 phylogenies. We then made a consensus phylogeny from the seven using the IQtree '-con' command.

379 We also reconstructed an unrooted phylogeny following the protocol from von Seth et al. (2022).
380 We used ngsDist (Vieira et al. 2015) to estimate a genetic distance matrix with 1000 bootstrap replicates
381 from the genotypes allowing no missing data. We then used FASTME v2.1.6.2 (Lefort et al. 2015) to
382 reconstruct the phylogeny, adding bootstrap support to the nodes using RAxML-ng v1.0.1 (Kozlov et al.
383 2019).
384

385 **Principal component analysis, genetic diversity, and introgression measurements**

386 We used Plink version 1.9 (Purcell et al., 2007) to convert the VCF file with the 66 caribou and no missing
387 data into a BED file. We then pruned the dataset to remove sites with a correlation co-efficient of 0.1 or
388 above in sliding windows of 50 SNPs, leaving 3,916,295 putatively unlinked SNPs, and then ran a PCA also
389 in plink, and plotted in R studio version 1.2.5041.
390 To estimate individual genetic diversity, we used mlRho v2.9 (Haubold et al. 2010) to calculate
391 heterozygosity for each individual from the bam files. mlRho calculates θ, an estimator of the population
392 mutation rate which approximates heterozygosity under the infinite sites model (vonSeth et al. 2022;
393 Haubold et al. 2010; Foote et al. 2021). The files were first filtered using Samtools to remove bases with
394 a mapping quality below 30, sites with a base quality below 30, and with a depth over 10X the average
395 for the dataset.
396 We measured introgression using ABBA BABA tests to control for incomplete lineage sorting. We
397 used Dsuite version 0.5 (Malinsky et al., 2021) to run the 'Dtrios' function to calculate D and f4-ratio
398 statistics, grouping our individuals by the lineages uncovered in our phylogenomic analysis (see results),
399 using the phylogeny as input using the '-t' command. When groups share branches on a phylogeny, many
400 elevated D and f4-ratio statistics can occur, however these correlated statistics can be informative to
401 uncover the relative time of the gene flow events across the phylogeny and to discover whether the
402 gene flow occurred on internal branches by using the f-branch statistic (Malinsky et al., 2021). We

403 calculated the f-branch statistics using the output from Dtrios, and then plotted alongside the phylogeny
404 using the 'dtools.py' script included with DSuite, setting the p-value to 0.05.
405 As these statistics are unable to measure gene flow between sister groups, we used SplitsTree
406 (Hudson and Bryant, 2006) to visualize the phylogenetic network as an 'admixture graph', using the
407 seven files SplitsTree output by IQtree (one for each of the 300 million base pair phylogenomic analyses).
408

409 **Rapidly evolving genes and gene ontology analysis**

410 We used GWideCodeML (Macías et al., 2020), a python package to run the codeml function of PAML
411 (Yang, 2007) in a computationally efficient way using genome-wide data. We used our annotation file to
412 extract all genes from the genomes of our individuals to use in GWideCodeML. To do this, we made a
413 consensus fasta file for each individual in the VCF file with our 66 caribou filtering to remove sites with
414 more than 5% missing data, as described above. We then used the '-x' function in Gffread version 0.12.3
415 (Pertea & Pertea, 2020) which pulls out the coding sequence for each gene as indicated in the
416 annotation file and splices them together (to remove introns), to create one fasta file per individual with
417 all genes. We reformatted the files so each gene sequence is on one line using 'awk' commands, and
418 then renamed the header line of each gene to include the ID of each individual (in addition to the gene
419 ID from the annotation) using 'sed' commands. We used the 'CSplit' command to split the files into one
420 file per gene, and then concatenated the files for each gene – resulting in one file per gene containing
421 the sequence for all 66 individuals.
422 We first ran the genes using an unrooted version of the tree as required by codeml. We removed
423 the outgroup reindeer and then used the 'ape' package in R studio to transform the tree into an
424 unrooted version with a trifurcation at the root, the format needed by codeml. We used the branch
425 model, which uses a Likelihood Ratio Test (LRT) to test whether the genes have a significantly different
426 dN/dS ratio on the focal branch, compared to all other branches of the tree. We tested this for each of

427 the nine major lineages uncovered in our phylogenomic analysis, excluding one individual, the boreal
428 caribou from Alberta, which is a hybrid between the NAL and BEL lineages as indicated by the PCA
429 analysis (Supplementary Figure 3). We then performed a Bonferroni multiple testing correction on the
430 Likelihood ratio results, adjusting the significance threshold to account for running the model over nine
431 lineages. We then took those sites where the focal branch was putatively under positive selection (larger
432 dN/dS ratio), and as some genes can be significant in multiple branches, we also calculated how many
433 genes were unique to each branch. We then used a chi-squared test in R studio to determine if there
434 were a significantly different number of positively selected genes across the different lineages.
435 To assign putative functions to the significant genes (after Bonferroni correction), we used
436 ShinyGo v0.76.2 (Ge et al., 2020) and assigned functions based on the GO Biological Process and GO
437 Molecular Function databases. The enrichment analysis outputs any biological pathways over-
438 represented in the list of genes with signatures of positive selection, and was performed for the
439 significant rapidly evolving genes for each of the nine major lineages separately.
440

441 **Runs of homozygosity (ROH) estimation**

442 To estimate the proportion of the genome in ROH we used Plink from the VCF file with no missing data
443 and not LD pruned, and only using scaffolds 1-35 to ensure removing sex chromosomes as above. To test
444 the impact of the key settings (homozyg-snp, homozyg-density, homozyg-gap, homozyg-window-snp,
445 homozyg-window-het, homozyg-het) on the resulting data, we ran 11 different combinations to optimize
446 the runs (Supplementary Material: ROH Plink Settings). Due to our high coverage (over 15X as
447 recommended for this analysis in Plink) and very high SNP density dataset (an average of ~1 SNP every
448 125 bp) many of the settings did not affect the results and for those that did we chose a conservative
449 approach (results for all runs available Supplementary Material: ROH Plink Settings) and landed on final
450 settings of homozyg-snp 100, homozyg-density 20, homozyg-gap 1000, homozyg-window-snp 100,

homozyg-window-het 1, homozyg-window-missing 5, and homozyg-het 3. Homozyg-kb and homozyg-window-threshold were set using recommendations from Meyermans et al. (2020), so using a homozyg-kb set the same as the scanning window size (100) and using their formula setting homozyg-window-threshold to 0.05.

**Mutational load**

We used two approaches to estimate mutational load, one annotation free method and one using our new annotation, to ensure concordance of our results using different approaches and in case of any bias arising from the annotation. For this, we used both genomic evolutionary rate profiling (GERP) analysis (Davydov et al. 2010) and SnpEff (Cingolani et al. 2012) which used our new annotation. For the GERP analysis we largely followed the protocol from von Seth et al. (2022). Firstly, we generated a TimeTree phylogeny (http://www.timetree.org/) of 48 mammal species (Supplementary Figure 8) representing those with available genomes from the even-toed and odd-toed ungulates due to turnover of constrained sites over larger phylogenetic distances (Huber et al. 2020). We downloaded the reference genomes for each of the 48 species and converted to fastq format using BBmap v38.86 (Bushnell et al. 2017), and then aligned to the caribou reference genomes using BWA-MEM (Li, 2013). We converted the resulting alignment files to BAM format and filtered them to remove reads aligning to more than one location as well as supplementary reads, and sorted the resulting file. We then used htsbox (https://github.com/lh3/htsbox) with quality filters (-R -q 30 -Q 30 -l 35 -s 1) to convert into fasta format, and the split each file to make one file per scaffold for the first 36 scaffolds (~99% of the genome assembly) which were then concatenated together to make one fasta alignment file for each scaffold with all species.

473 The resulting alignment files were run through a modified version of the gerpcol function in
474 GERP (tar file available here: https://github.com/BeckySTaylor/Phylogenomic_Analyses). Because it can
475 lead to biases (Wootton et al. 2023) the focal species, here caribou, should not be included in the GERP
476 analysis. However, this leads to missing data in the alignment which makes it difficult to interpret the
477 output files which don't print which site the score pertains to. We modified the code for the gerpcol
478 function to print out the position for each score, as well as the allele for the specified sister species, here
479 the white-tailed deer, which is used as the ancestral allele for each site. This was run using a Ts/Tv ratio
480 of 2.06 as calculated in BCFtools for our caribou dataset. Additionally, as the TimeTree phylogeny outputs
481 the branch lengths in millions of years but gercol requires substitutions per site, we used a tree scaling
482 factor (-s) of 0.0022 reflecting the number of mutations per million years on average per site based on
483 the average mammal mutation rate of $2.2 \times 10{-}9$ (Kumar and Subramian, 2002). We then wrote a
484 custom R script (available here: https://github.com/BeckySTaylor/Phylogenomic_Analyses) to automate
485 taking the output and extracting the derived alleles at all sites with positive scores, as well as all sites
486 with a score over 2 (representing the top portion of the possible score range which is a maximum of 2.46
487 for our dataset and therefore the most highly constrained sites) from our 66 caribou genomes using the
488 VCF file with no missing data.

489 To get another measure of mutational load, we ran SnpEff using our new annotation and then
490 pulled out SNPs labelled as loss of function (LOF), high impact (which includes the LOF), moderate
491 impact (e.g. missense variants), and low impact (e.g. synonymous variants). We extracted derived SNPs
492 only using the white-tailed deer as an outgroup using the same custom R script as above from the GERP
493 analysis.

494

495 **Data and code availability**

496 Whole genome sequences from 50 samples used for this study are available on the National Centre for
497 Biotechnology (NCBI) under BioProject Accession numbers PRJNA634908, PRJNA694662, PRJNA754521,
498 and PRJNA984705. The sequences for the new genomes, and the new reference genome assembly and
499 annotation, will be made available upon acceptance. Bioinformatic code used in this study is available at:
500 https://github.com/BeckySTaylor/Phylogenomic_Analyses

501

502 **Acknowledgments**

503 We would like to thank the many field collectors and hunters who supplied samples for this work, as well
504 as Bridget Redquest and Austin Thompson for technical support in the laboratory. We would also like to
505 thank Brody Crosby for support with data management, and other members of the Ecogenomics team
506 (https://www.ecogenomicscanada.ca/) for the many insightful conversations. We are also thankful to the
507 Shared Hierarchical Academic Research Computing Network (SHARCNET: www.sharcnet.ca), Compute
508 Canada, and Amazon Cloud Computing for high-performance computing services. Funding from this
509 research was provided by the Genomic Applications Partnership Program of Genome Canada,
510 Environment and Climate Change Canada, the Government of Canada's Genomics Research and
511 Development Initiative (GRDI), the Species-at-Risk Stewardship Program (SARSP), WCS Garfield Weston
512 Fellowship. We would also like to thank Lukas Keller and two anonymous reviewers for their feedback on
513 the manuscript.

514

515 **Author contributions**

516 R.S.T. helped to conceive the study, did the bioinformatics, and wrote the manuscript. M.M. helped to
517 conceive the study, secured funding, and edited the manuscript. S.K. helped with the bioinformatics and

518 edited the manuscript, P.L. wrote scripts for some bioinformatic analyses, and G.M. did the laboratory
519 work to produce the fibroblast cells for the reference genome and annotation. K.S. secured funding and
520 support with bioinformatics, A.K., N.C.L., M.G., H.S., C.T., J.P., L.A., D.H., and D.S. coordinated or collected
521 samples and edited the manuscript. P.J.W. helped to conceive the study, secured funding, and edited the
522 manuscript.

523

524 **Declaration of interests**

525 The authors declare no competing interests.

526

527 **References**


528 1. Hoban, S. et al. Global genetic diversity status and trends: towards a suite of Essential
529 Biodiversity Variables (EBVs) for genetic composition. *Biol. Rev.* **97**, 1511-1538 (2022).
530 2. Andrello, M. et al. Evolving spatial conservation prioritization with intraspecific genetic
531 data. *TREE* **37**, 553–564 (2022).
532 3. Carvalho, S. B. et al. Spatial conservation prioritization of biodiversity spanning the evolutionary
533 continuum. *Nat. Ecol. Evol.* **1**, 0151 (2017).
534 4. O'Brien, D. et al. Bringing together approaches to reporting on within species genetic diversity. *J.*
535 *Appl. Ecol.* ***59*****,** 2227-33 (2022).
536 5. Des Roches, S., Pendleton, L. H., Shapiro, B., & Palkovacs, E. P. Conserving intraspecific variation
537 for nature's contributions to people. *Nat. Ecol. Evol.* **5**, 574-82 (2021).
538 6. Leigh, D. M. et al. Opportunities and challenges of macrogenetic studies. *Nat. Rev. Genet.* **22**,
539 791–807 (2021).

7. Yiming, L. et al. Latitudinal gradients in genetic diversity and natural selection at a highly adaptive gene in terrestrial mammals. *Ecography* **44**, 206–218 (2021).
8. Bertorelle, G. et al. Genetic load: genomic estimates and applications in non-model animals. *Nat. Rev. Genet*. **23**, 492–503 (2022).
9. van Oosterhout, C. et al. Genomic erosion in the assessment of species extinction risk and recovery potential. Preprint at: Genomic erosion in the assessment of species extinction risk and recovery potential | bioRxiv (2022).
10. von Seth, J. et al. Genomic insights into the conservation status of the world's last remaining Sumatran rhinoceros populations. *Nat. Comms*. **12**, 2393 (2022).
11. Dussex, N. et al. Population genomics of the critically endangered kākāpō. *Gell Genomics* **1**, 100002 (2021).
12. Grossen, C., Guillaume, F., Keller, L. F. & Croll, D. Purging of highly deleterious mutations through severe bottlenecks in Alpine Ibex. *Nat. Comms*. **11**, 1001 (2020).
13. Khan, A. et al. Genomic evidence for inbreeding depression and purging of deleterious genetic variation in Indian tigers. *PNAS* **118**, e2023018118 (2021).
14. Kardos, M. et al. Inbreeding depression explains killer whale population dynamics. *Nat. Ecol. Evol.* **7**, 675-686 (2023).
15. Smeds, L. & Ellegren, H. From high masked to high realized genetic load in inbred Scandinavian wolves. *Mol. Ecol.* **32**, 1567-1580 (2022).
16. Fairmount, A., Rastas, P., Lv, L. & Merila. Inbreeding depression in an outbred stickleback population. Mol. Ecol. (2023).
17. COSEWIC. Designatable units for caribou (*Rangifer tarandus*) in Canada. Committee on the Status of Endangered Wildlife in Canada (2011).

563 18. Festa-Bianchet, M., Ray, J. C., Boutin, S., Côté, S. D. & Gunn, A. Conservation of caribou (*Rangifer*
564 *tarandus*) in Canada: An uncertain future. *Can. J. Zool.* **89**, 419–434 (2011).
565 19. Vors, L. S. & Boyce, M. S. Global declines of caribou and reindeer. *Global Change Biol.* **15**, 2626–
566 2633 (2009).
567 20. Weckworth, B. V., Hebblewhite, M., Mariani, S. & Musiani, M. Lines on a map: Conservation
568 units, meta-population dynamics, and recovery of woodland caribou in Canada. *Ecosphere* **9**,
569 e02323 (2018).
570 21. COSEWIC. COSEWIC assessment and status reports available Document search - Species at risk
571 registry (canada.ca)
572 22. Gunn, A. *Rangifer tarandus*. The IUCN Red List of Threatened Species 2016: e.T29742A22167140
573 (2016). Accessed on 10 June 2023.
574 23. Gripenberg, U. & Nieminen, M. The chromosomes of reindeer (*Rangifer tarandus*). *Rangifer* **6**,
575 109 (1986).
576 24. Weckworth, B. V., McDevitt, A., Musiani, M., Hebblewhite, M. & Mariani, S. Reconstruction of
577 caribou evolutionary history in Western North America and its implications for conservation.
578 *Mol. Ecol.* **21**, 3610–3624 (2012).
579 25. Haubold, B., Pfaffelhuber, P. & Lynch, M. mlRho – a program for estimating the population
580 mutation and recombination rates from shotgun-sequenced diploid genomes. *Mol. Ecol*. **19**, 277-
581 284 (2010).
582 26. Foote, A. D. et al. Runs of homozygosity in killer whale genomes provide a global record of
583 demographic histories. *Mol. Ecol.* **30**, 6162-6177 (2021).
584 27. Morin P. A. et al. Reference genome and demographic history of the most endangered marine
585 mammal, the vaquita. *Mol. Ecol. Resour*. **21**, 1008-1020 (2020).

586 28. Polfus, J. L., Manseau, M., Klütsch, C. F. C., Simmons, D. & Wilson, P. J. Ancient diversification in
587 glacial refugia leads to intraspecific diversity in a Holarctic mammal. *J. Biogeog.* **44**, 386–396
588 (2017).
589 29. Taylor. R. S. et al. Population dynamics of caribou shaped by glacial cycles before the last glacial
590 maximum. *Mol. Ecol.* **30**, 6121–6143 (2021).
591 30. Boulet, M., Couturier, S., Cote, S. D., Otto, R. D. & Bernatchez, L. Integrative use of spatial,
592 genetic, and demographic analyses for investigating genetic connectivity between migratory,
593 montane, and sedentary caribou herds. *Mol. Ecol.* **20**, 4223-40 (2007).
594 31. McLoughlin, P. D., Paetkau, D., Duda, M. & Boutin, S. Genetic diversity and relatedness of boreal
595 caribou populations in western Canada. *Biol. Conserv.* **118**, 593–598 (2004).
596 32. Zittlau, K., Coffin, J., Farnell, R., Kuzyk, G. & Strobeck, C. Genetic relationships of three Yukon
597 caribou herds determined by DNA typing. *Rangifer* **12**, 59–62 (1998).
598 33. Galbreath, K. E., Cook, J. A., Eddingsaas, A. A. & DeChaine, E. G. Diversity and demography in
599 Beringia: Multilocus tests of paleodistribution models reveal the complex history of Arctic
600 ground squirrels. *Evolution* **65**, 1879–1896 (2011).
601 34. Dussex, N. et al. Moose genomes reveal past glacial demography and the origin of modern
602 lineages. *BMC Genomics* **21**, 854 (2020).
603 35. Roberts, D. R. & Hamann, A. Glacial refugia and modern genetic diversity of 22 western North
604 American tree species. *Proceedings R. Soc. B: Biol. Sci.* **282**, 20142903 (2015).
605 36. Petit, R. J. et al. Glacial refugia: hotspots but not melting pots of genetic diversity. *Science* **300**,
606 1563–1565 (2003).
607 37. Alcala, N. & Vuilleumier, S. Turnover and accumulation of genetic diversity across large time-
608 scale cycles of isolation and connection of populations. *Proceedings R. Soc. B: Biol. Sci.* **281**,
609 20141369 (2014).

610 38. Maier, P. A., Vandergast, A. G., Ostoja, S. M., Aguilar, A. & Bohonak, A. J. Pleistocene glacial cycles
611 drove lineage diversification and fusion in the Yosemite toad (*Anaxyrus canorus*). *Evolution* **73**,
612 2476-96 (2019).
613 39. Berner, D. & Salzburger, W. The genomics of organismal diversification illuminated by adaptive
614 radiations. *Trends Genet.* **31***,* 491–499 (2015).
615 40. Latch, E. K., Heffelfinger, J. R., Fike, J. A. & Rhodes Jr, O. E. Species-wide phylogeography of North
616 American mule deer (*Odocoileus hemionus*): cryptic glacial refugia and postglacial recolonization.
617 *Mol. Ecol.* **18**, 1730-45 (2009).
618 41. Yang, Z. PAML 4: phylogenetic analysis by maximum likelihood. *Mol. Biol. Evol.* **24**, 1586-91
619 (2007).
620 42. Weldenegodguad, M. et al. Adipose gene expression profiles reveal insights into the adaptation
621 of northern Eurasian semi-domestic reindeer. *Comms. Biol*. **4**, 1170 (2021).
622 43. Streicher, J. W. et al. Diversification and asymmetrical gene flow across time and space: lineage
623 sorting and hybridization in polytypic barking frogs. *Mol. Ecol.* **23**, 3273–3291 (2014).
624 44. Lexer, C et al. Gene flow and diversification in a species complex of *Alcantarea* inselberg
625 bromeliads. *Botan. J. Linn. Soc.* **181**, 505–520 (2016).
626 45. Solmundson, K. et al. Whole genomes reveal caribou population structure and inbreeding
627 histories. *Ecol. Evol*. **13**, e10278 (2023)
628 46. Seip, D. R. & Cichowski, D. B. Population Ecology of caribou in British Columbia. *Rangifer*, **9**, 73-
629 80 (1996).
630 47. Ministry of Forests, Lands, Natural Resource Operations and Rural Development. Itcha-Ilgachuz
631 and Rainbow caribou herd population and habitat information. 54951 (2018).

632 48. Cuyler, C., Rosing, M., Linnell, J. D. C., Loison, A., Ingerslev, T. & Landa, A. Status of the
633 Kangerlussuaq-Sisimiut caribou population (*Rangifer tarandus groenlandicus*) in 2000, West
634 Greenland. Greenland Institute of Natural Resources, Technical Report No. 42 (2002).
635 49. Davydov, E. V. et al. Identifying a high fraction of the human genome to be under selective
636 constraint using GERP++. *PLoS Comput. Biol.* **6**, e1001025 (2010).
637 50. Dussex, N., Morales, H. E., Grossen, C., Dalén, L. & van Oosterhout, C. Purging and accumulation
638 of genetic load in conservation. TREE (2023).
639 51. Hanson, J. O., Fuller, R. A. & Rhodes, J. R. Conventional methods for enhancing connectivity in
640 conservation planning do not always maintain gene flow. *J. Appl. Ecol.* **56**, 913–922 (2019).
641 52. Mathur, S. et al. An evolutionary perspective on genetic load in small isolated populations as
642 informed by whole genome resequencing and forward-time simulations. *Evolution* **77**, 690-704
643 (2023).
644 53. Kleinman-Ruiz, D. et al. Purging of deleterious burden in the endangered Iberian lynx. *PNAS* **119**,
645 e2110614119 (2022).
646 54. Xie, H. et al. Ancient demographics determine the effectiveness of genetic purging in
647 endangered lizards. *Mol. Biol. Evol.* **39**, msab359 (2021).
648 55. Taylor, R. S. et al. The caribou (*Rangifer tarandus*) genome. *Genes 10*, 540 (2019).
649 56. Putnam, N. H. et al. Chromosome-scale shotgun assembly using an in vitro method for long-
650 range linkage. *Genome Res.* **26**, 342–350 (2016).
651 57. Yamaguchi, K. et al. Technical considerations in Hi-C scaffolding and evaluation of
652 chromosome-scale genome assemblies. *Mol. Ecol.* **30**, 5923-34 (2021).
653 58. Taylor, R. S. et al. The role of introgression and ecotypic parallelism in delineating intraspecific
654 conservation units. *Mol. Ecol.* **29**, 2793–2809 (2020).

655 59. Taylor, R. S. et al. Whole genome sequences from non-invasively collected caribou faecal
656 samples. *Conserv. Genet. Resour.* **14**, 53-68 (2022).
657 60. Bolger, A. M., Lohse, M. & Usadel, B. trimmomatic: A flexible trimmer for Illumina sequence
658 data. *Bioinformatics* **30**, 2114–2120 (2014).
659 61. Langmead, B. & Salzberg, S. L. Fast gapped-read alignment with bowtie 2. *Nature Methods* **9**,
660 357–359 (2012).
661 62. Li, H., et al. The sequence alignment/map format and samtools. *Bioinformatics* **25**, 2078–2079
662 (2009).
663 63. McKenna, A. et al. The genome analysis toolkit: A MapReduce framework for analyzing next-
664 generation DNA sequencing data. *Genome Rese. 20*, 1297–1303 (2010).
665 64. Danecek, P. et al. The variant call format and VCFtools. *Bioinformatics* **27**, 2156–2158 (2011).
666 65. Weldenegodguad, M. et al. Genome sequence and comparative analysis of reindeer (*Rangifer*
667 *tarandus*) in northern Eurasia. *Sci. Rep.* **10**, 1-4 (2020).
668 66. Nguyen, L-T., Schmidt, H. A., von Haeseler, A. & Minh, B. Q. IQ-TREE: A fast and effective
669 stochastic algorithm for estimating maximum likelihood phylogenies. *Mol. Biol. Evol.* **32**, 268-274
670 (2015).
671 67. Galloway, S. M. et al. A linkage map of the ovine X chromosome. *Genome Res.* **6**, 667–677
672 (1996).
673 68. Liu, R. et al. New insights into mammalian sex chromosome structure and evolution using high-
674 quality sequences from bovine X and Y chromosomes. *BMC Genomics* **20**, 1000 (2019).
675 69. Hoang, D. T., Chernomor, O., von Haeseler, A., Minh, B. Q. & Vinh, L. S. UFBoot2: Improving the
676 ultrafast bootstrap approximation. *Mol. Biol. Evol.* **35**, 518–522 (2018).
677 70. Vieira, F. G., Lassalle, F., Korneliussen, T. S. & Fumagalli, M. Improving the estimation of genetic
678 distances from Next-Generation Sequencing data. Biol. J. Linn. Soc. 117, 139-149 (2015).

679 71. Lefort, V., Desper, R. & Gascuel, O. FastME 2.0: A Comprehensive, Accurate, and Fast Distance-
680 Based Phylogeny Inference Program. *Mol. Biol. Evol.* **32**, 2798–2800 (2015).
681 72. Kozlov, A. M., Darriba, D., Flouri, T., Morel, B. & Stamatakis, A. RAxML-NG: a fast, scalable and
682 user-friendly tool for maximum likelihood phylogenetic inference. *Bioinformatics* **35**, 4453–4455
683 (2019).
684 73. Purcell, S. et al. plink: A tool set for whole-genome association and population-based linkage
685 analyses. *Am. J. Human Genet.* **81**, 559–575 (2007).
686 74. R Core Team. R: A language and environment for statistical computing. R Foundation for
687 Statistical Computing (2018).
688 75. Malinsky, M., Matschiner, M. & Svardal, H. dsuite – Fast D statistics and related admixture
689 evidence from VCF files. *Mol. Ecol. Resour.* **21**, 584–595 (2021).
690 76. Hudson, D. H. & Bryant, D. Application of phylogenetic networks in evolutionary studies. *Mol.*
691 *Biol. Evol.* **23**, 254-67 (2006).
692 77. Macías, L. G., Barrio, E. & Toft, C. GWideCodeML: a python package for testing evolutionary
693 hypotheses at the genome-wide level. *G3: Genes, Genomes, Genet.* **10**, 4369-72 (2020).
694 78. Pertea, G. & Pertea, M. GFF utilities: GffRead and GffCompare. *F1000Research,* **9** (2020).
695 79. Ge, S.X., Jung, D. & Yao, R. ShinyGO: a graphical gene-set enrichment tool for animals and plants.
696 *Bioinformatics* **36**, 2628-9 (2020).
697 80. Meyermans, R., Gorssen, W., Buys, N & Janssens, S. How to study runs of homozygosity using
698 PLINK? A guide for analyzing medium density SNP data in livestock and pet species. *BMC Genom*.
699 **21**, 94.
700 81. Cingolani, P. et al. A program for annotating and predicting the effects of single nucleotide
701 polymorphisms, SnpEff: SNPs in the genome of Drosophila melanogaster strain w1118; iso-2;
702 iso-3. *Fly 6*, 80–92 (2012).

703 82. Huber, C. D., Kim, B. Y. & Lohmueller, K. E. Population genetic models of GERP scores suggest
704 pervasive turnover of constrained sites across mammalian evolution. *Plos Genet*. **16**, e1008827
705 (2020).
706 83. Bushnell, B., Rood, J. & Singer, E. BBMerge—Accurate paired shotgun read merging via
707 overlap. *PLoS ONE,* **12**, e0185056 (2017).
708 84. Li H. (2013) Aligning sequence reads, clone sequences and assembly contigs with BWA-MEM.
709 Preprint at arXiv:1303.3997v2
710 85. Wootton, E., Robert, C., Taillon, J., Côté, S. D. & Shafer, A. B. A. Genomic health is dependent on
711 long-term population demographic history. *Mol. Ecol.* **32**, 1943– 1954 (2023).
712 86. Kumar, S. & Subramian, S. Mutation rates in mammalian genomes. *PNAS* **99**, 803-808 (2002).

713

714

715 **Figure legends**

716 **Figure 1. Map of sampled individuals.** A map showing the sample location of each of the individuals
717 sequenced. The background shading indicates the Designatable Unit (DU) ranges and the colours of the
718 points indicate which phylogenomic lineage the individual belongs to.

719 **Figure 2. Intra-specific diversity of caribou. a**, simplified version of the whole genome phylogenomic
720 reconstruction showing which caribou belong to each lineage. **b**, Genetic diversity (θ) for each lineage.

721 **Figure 3. Levels of introgression between lineages and their number of enriched functional pathways.**
722 **a,** heatmap showing the f-Branch statistics alongside the phylogeny. The gene flow is from the lineage
723 indicated in the top phylogeny (X-axis) going into the phylogeny represented on the Y-axis. Dotted lines
724 indicate where gene flow is going into an ancestral group on the phylogeny. Greyed out squares indicate

725 tests that could not be made with this statistic, and white squares indicate where no gene flow was
726 detected. **b**, the number of enriched functional pathways within each lineage, under the categories
727 biological processes and molecular function, from their rapidly evolving genes.

728 **Figure 4. Inbreeding extent in the caribou lineages. a,** FROH, or the proportion of the genome in runs of
729 homozygosity, **b**, the number of runs of homozygosity in total, **c**, the number of runs of homozygosity up
730 to one million base pairs, and **d**, the number of runs of homozygosity over one million base pairs. The
731 outlier dots for the ARC lineage (**a-c**) are the Kangerlussuaq caribou from Greenland.

732 **Figure 5. Genetic load as profiled using genomic evolutionary rate profiling (GERP). a,** the number of
733 derived alleles with a positive GERP score for each lineage and **b**, the average GERP score for the derived
734 alleles with positive scores for each lineage. **c**, the number of derived alleles with a GERP score over two
735 for each lineage and **d**, the average GERP score for the derived alleles scores over two for each lineage.

736 **Figure 6. Genetic load as profiled using the genome annotation**. The number of derived loss of function,
737 high impact, moderate impact, and low impact alleles in each lineage (**a-d** respectively).

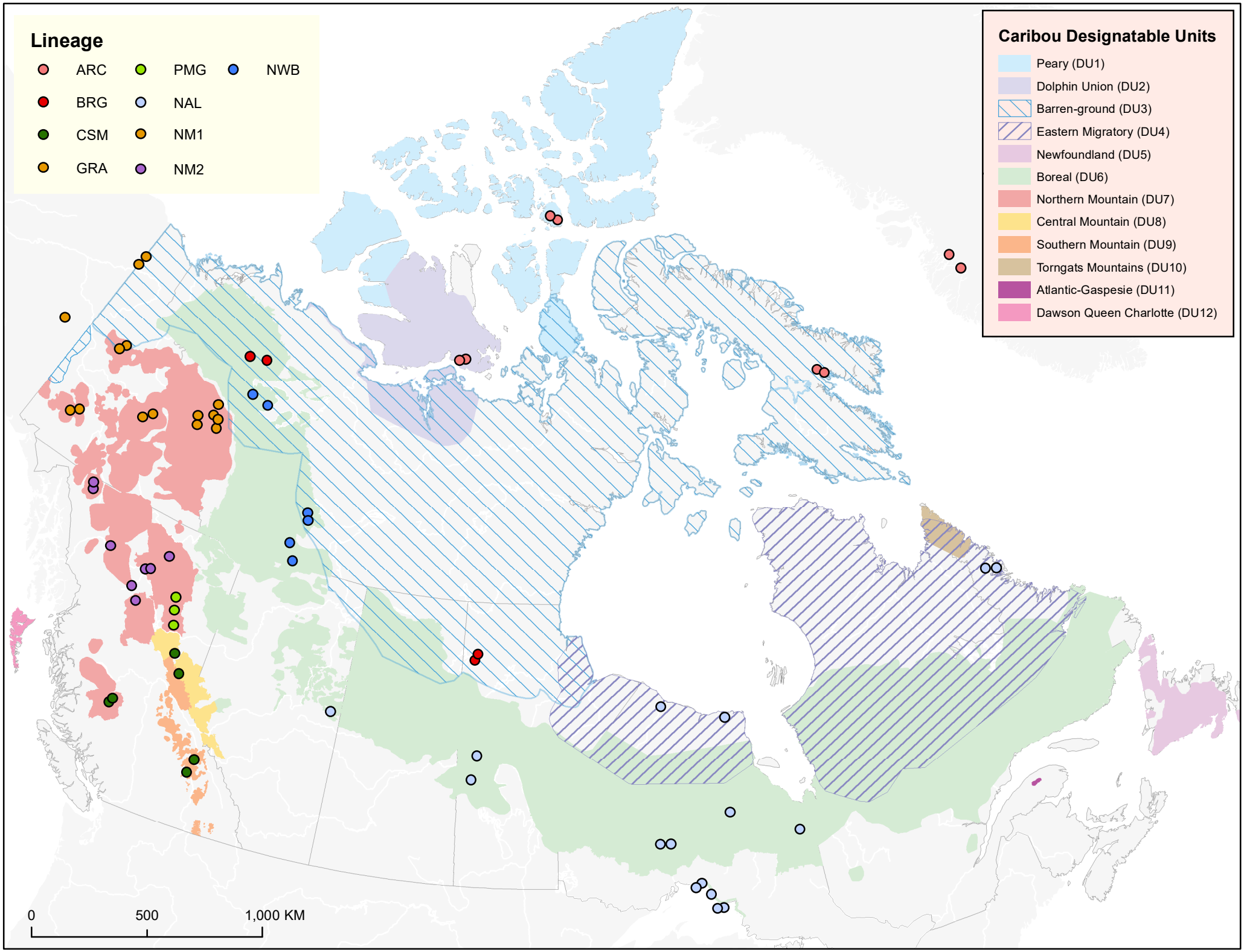
Lineage
ARC
PMG
NWB
BRG
NAL
CSM
NM1
GRA
NM2
Caribou Designatable Units
Peary (DU1)
Dolphin Union (DU2)
Barren-ground (DU3)
Eastern Migratory (DU4)
Newfoundland (DU5)
Boreal (DU6)
Northern Mountain (DU7)
Central Mountain (DU8)
Southern Mountain (DU9)
Torngats Mountains (DU10)
Atlantic-Gaspesie (DU11)
Dawson Queen Charlotte (DU12)
0
500
1,000 KM

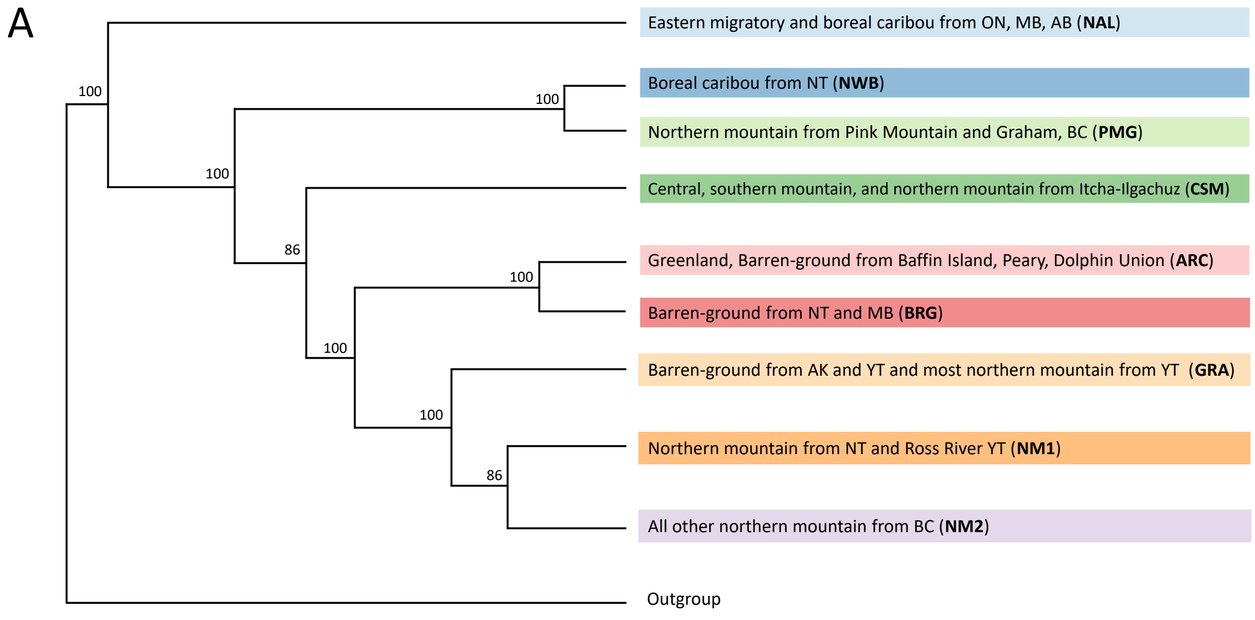
A
Eastern migratory and boreal caribou from ON, MB, AB (NAL)
Boreal caribou from NT (NWB)
Northern mountain from Pink Mountain and Graham, BC (PMG)
Central, southern mountain, and northern mountain from Itcha-Ilgachuz (CSM)
Greenland, Barren-ground from Baffin Island, Peary, Dolphin Union (ARC)
Barren-ground from NT and MB (BRG)
Barren-ground from AK and YT and most northern mountain from YT (GRA)
Northern mountain from NT and Ross River YT (NM1)
All other northern mountain from BC (NM2)
Outgroup
100
100
100
86
100
100
100
86

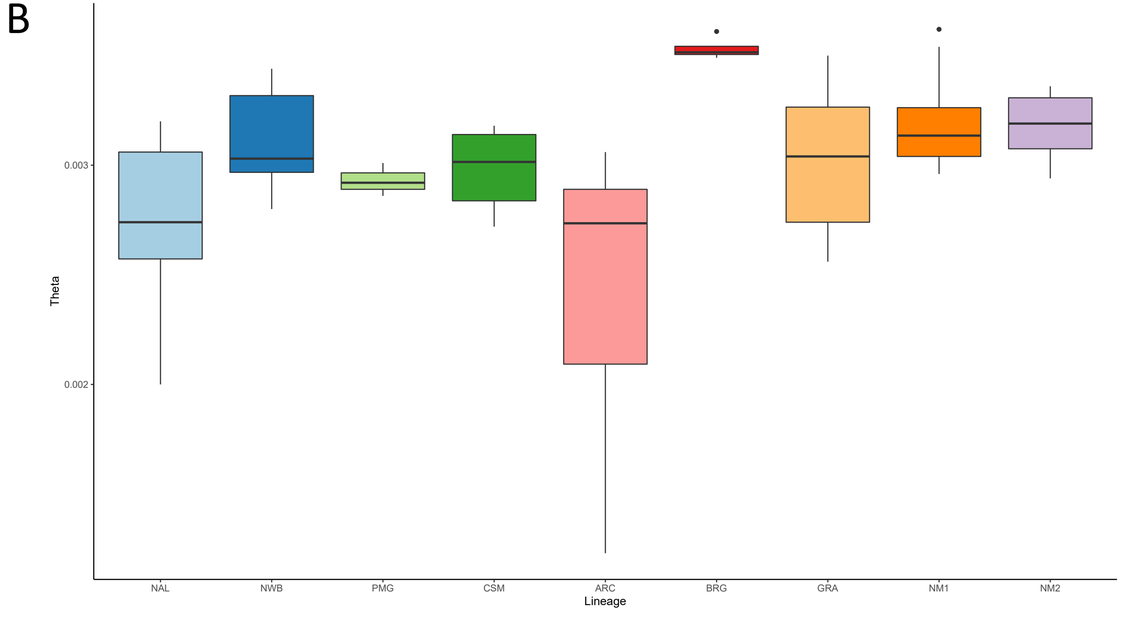
B
Theta
0.003
0.002
NAL
NWB
PMG
CSM
ARC
BRG
GRA
NM1
NM2
Lineage

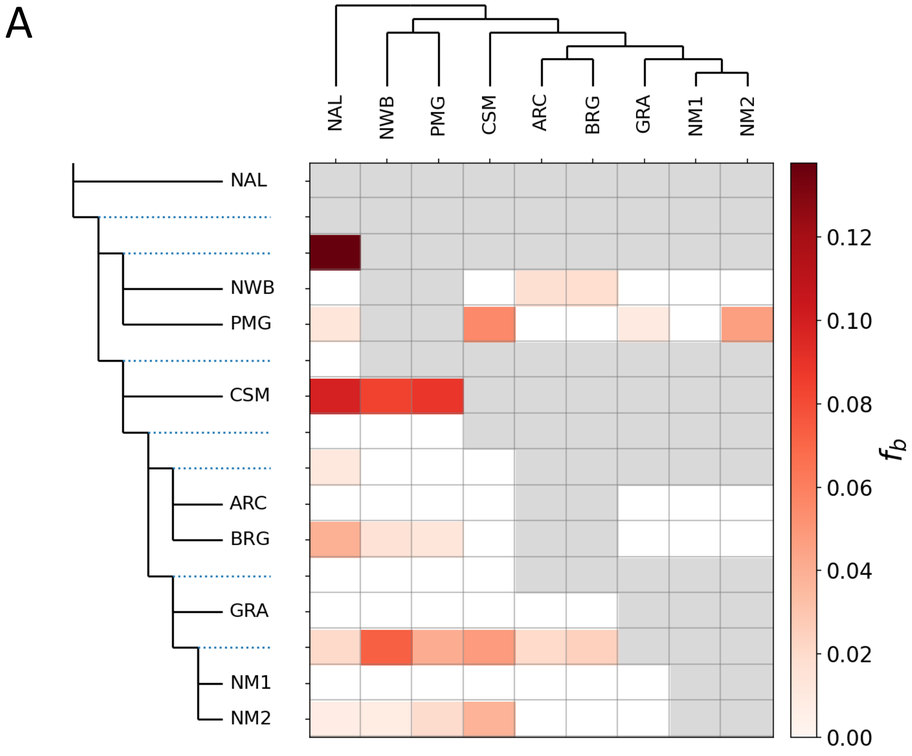
A
NAL
NWB
PMG
CSM
ARC
BRG
GRA
NM1
NM2
0.12
0.10
0.08
0.06
0.04
0.02
0.00
$f_b$

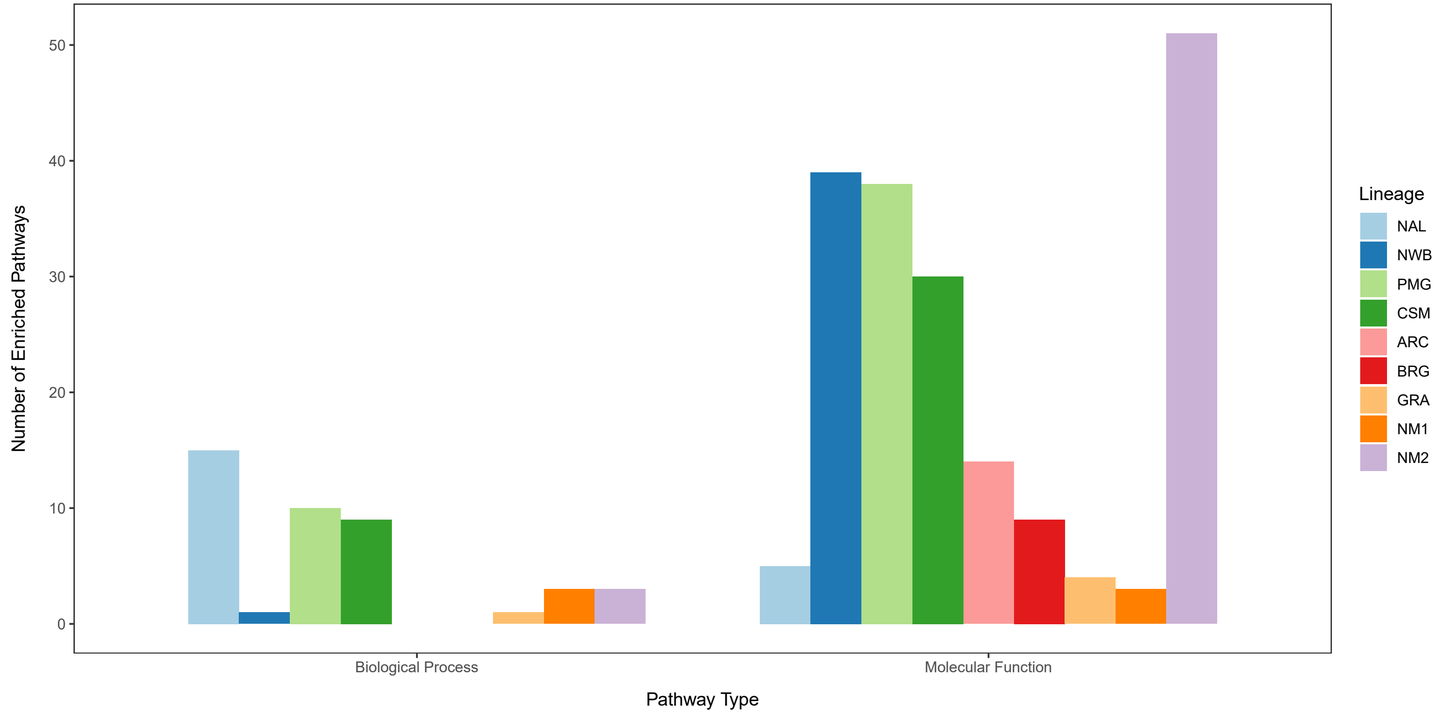
B
Number of Enriched Pathways
0
10
20
30
40
50
Biological Process
Molecular Function
Pathway Type
Lineage
NAL
NWB
PMG
CSM
ARC
BRG
GRA
NM1
NM2

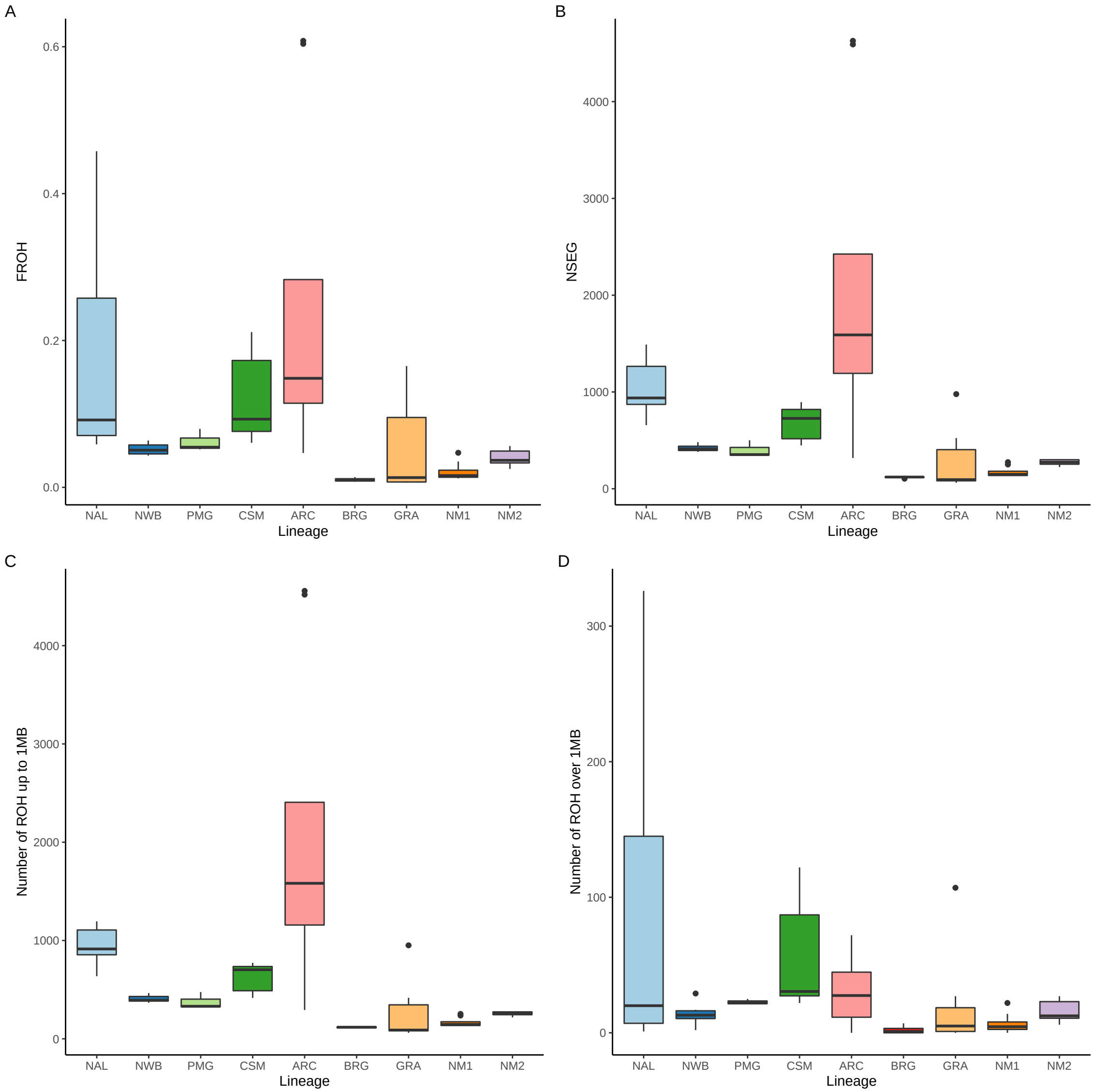
A
FROH
0.0
0.2
0.4
0.6
NAL
NWB
PMG
CSM
ARC
BRG
GRA
NM1
NM2
Lineage
B
NSEG
0
1000
2000
3000
4000
NAL
NWB
PMG
CSM
ARC
BRG
GRA
NM1
NM2
Lineage
C
Number of ROH up to 1MB
0
1000
2000
3000
4000
NAL
NWB
PMG
CSM
ARC
BRG
GRA
NM1
NM2
Lineage
D
Number of ROH over 1MB
0
100
200
300
NAL
NWB
PMG
CSM
ARC
BRG
GRA
NM1
NM2
Lineage

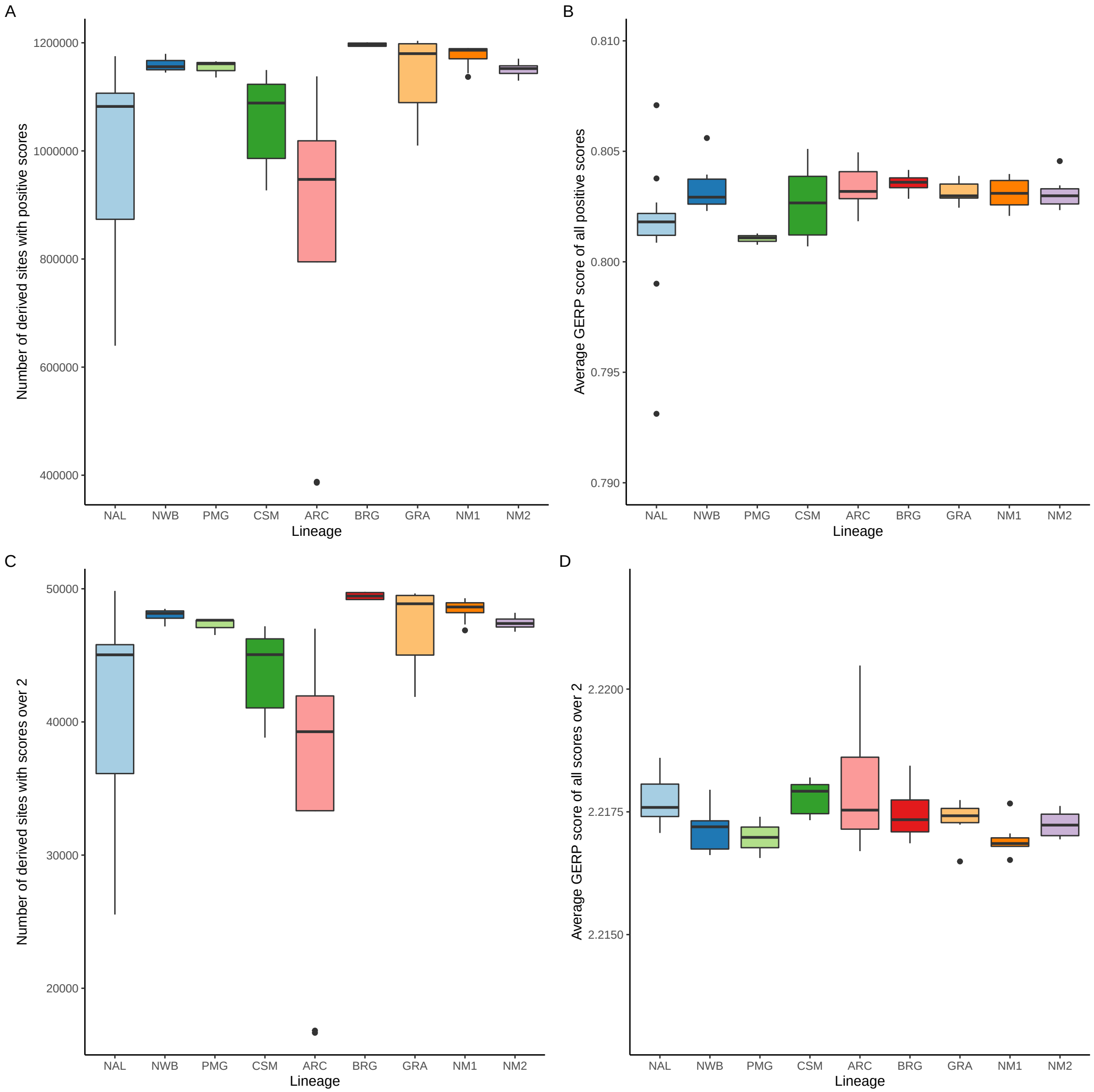
A
Number of derived sites with positive scores
1200000
1000000
800000
600000
400000
NAL
NWB
PMG
CSM
ARC
BRG
GRA
NM1
NM2
Lineage
B
Average GERP score of all positive scores
0.810
0.805
0.800
0.795
0.790
NAL
NWB
PMG
CSM
ARC
BRG
GRA
NM1
NM2
Lineage
C
Number of derived sites with scores over 2
50000
40000
30000
20000
NAL
NWB
PMG
CSM
ARC
BRG
GRA
NM1
NM2
Lineage
D
Average GERP score of all scores over 2
2.2200
2.2175
2.2150
NAL
NWB
PMG
CSM
ARC
BRG
GRA
NM1
NM2
Lineage

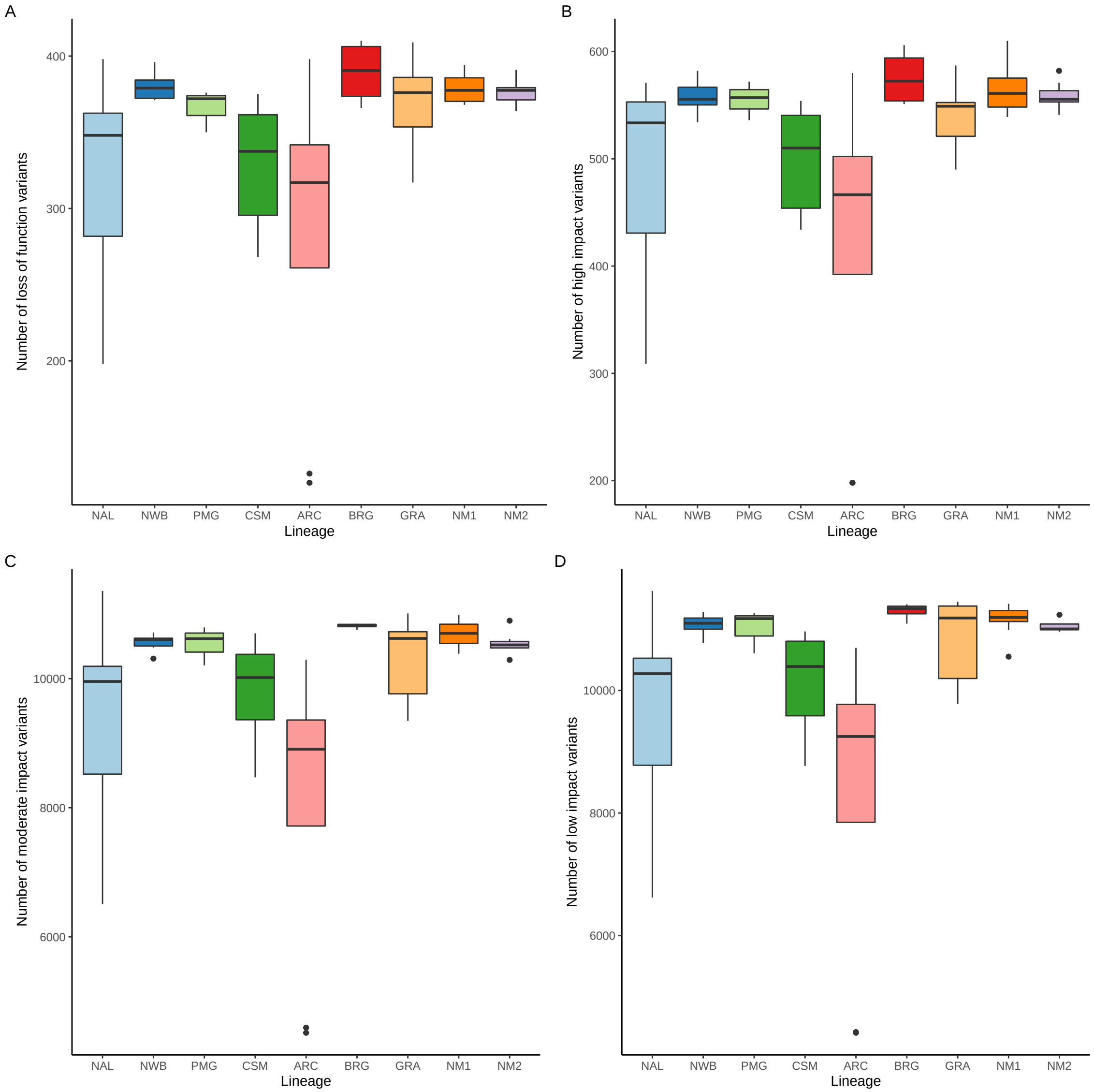
A
Number of loss of function variants
400
300
200
NAL
NWB
PMG
CSM
ARC
BRG
GRA
NM1
NM2
Lineage
B
Number of high impact variants
600
500
400
300
200
NAL
NWB
PMG
CSM
ARC
BRG
GRA
NM1
NM2
Lineage
C
Number of moderate impact variants
10000
8000
6000
NAL
NWB
PMG
CSM
ARC
BRG
GRA
NM1
NM2
Lineage
D
Number of low impact variants
10000
8000
6000
NAL
NWB
PMG
CSM
ARC
BRG
GRA
NM1
NM2
Lineage